Characterizing the Topological Properties of 1D Non-Hermitian Systems without the Berry–Zak Phase

Didier Felbacq, Emmanuel Rousseau

RESEARCH ARTICLE

annalen der physik
www.ann-phys.org

Characterizing the Topological Properties of 1D Non-Hermitian Systems without the Berry–Zak Phase

Didier Felbacq and Emmanuel Rousseau*

A new method is proposed to predict the topological properties of 1D periodic structures in wave physics, including quantum mechanics. From Bloch waves, a unique complex valued function is constructed, exhibiting poles and zeros. The sequence of poles and zeros of this function is a topological invariant that can be linked to the Berry–Zak phase. Since the characterization of the topological properties is done in the complex plane, it can easily be extended to the case of non-Hermitian systems. The sequence of poles and zeros allows to predict topological phase transitions.

1. Introduction

A considerable amount of work has been devoted to the study of the topological properties of photonic structures.[1] The word topological means that what is at stake are the properties of a structure that are stable under a continuous variation of the parameters defining it. For instance, the existence of a band gap is a topological property since a not too large variation of the properties (e.g., the size of the basic cell, the values of the electromagnetic parameters) does not close the gap. In some cases, the topological properties can be characterized by an integer number, a quantity that obviously remains constant over small continuous variations.[2] Of course, for larger variations it may happen that, for example, the gap closes, which can lead to a change in the integer number. This will be called a topological transition. First attempts to find topological properties in photonic structures were made by mimicking the field of topological insulators:[3] The time-reversal invariance was broken by the use of gyromagnetic materials controlled by a magnetic field. The devices considered there were quite complicated and specific. A major breakthrough was made when it was realized that topological effects could be obtained in purely dielectric structures.[4] As a matter of fact, a topological effect can be obtained for very simple structures: one dimensional stratified media exhibit boundary modes that are topologically protected.[5] These can be analyzed using theoretical tools that were developed a long time ago[6] and which have been given a second look in the context of geometric phases: in ref. [7], it was shown that the properties exhibited in ref. [6] could be interpreted using the mathematical apparatus developed by ref. [8] in view of the results obtained by Berry in ref. [9]. Mathematically speaking, this comes under the domain of vector bundles endowed with a connection.[10,11] Simon introduced in ref. [8] the now celebrated connection 1-form $A(k) = \langle u_k, \nabla_k u_k \rangle$, where u_k is a Bloch mode. This connection is often called the Berry connection, while it is in fact a specific case of the Levi–Civita connection.[12] Zak's article was probably the first work applying the concept of geometric phase to Bloch waves. Recently, there was an interest in the possibility of extending these results to non-Hermitian Hamiltonians[13–16] and, in the context of photonic crystals, to media with losses.[17] All the preceding results were obtained by generalizing the Levi–Civita connection for a non-Hermitian bundle. In the present work, we propose a new approach to the topological properties of 1D periodic structures. We show that the topological properties can be analyzed without reference to the Levi–Civita–Simon–Berry connection. We introduce a function of the wavenumber that presents poles and zeros. The arrangement of the poles and zeros characterizes the topological properties of the medium. It turns out that this pole and zero structure extends naturally to the situation when losses are present in the materials out of which the structure is made, that is to the non-Hermitian situation.

The article is organized as follows: In the first section, we recall the elements of the theory of wave propagation in 1D structures, comprising Bloch waves. In the second section, we develop our approach and introduce the function that will prove to be a clue to the understanding of the topological properties. In the third section, we make the link with the usual approach using the geometrical phase when the mediums under consideration are lossless. Finally, we extend the approach to the situation where loss is added. Throughout the sections, numerical illustrations are provided in order to clarify the somewhat abstract statements. Finally, in the conclusion, we show that our approach can also handle a structure with some disorder and comment on the extension to higher dimensions.

2. Wave Propagation in a 1D Structure

An example of a 1D medium is depicted in **Figure 1**. We have chosen to represent a 1D stratified photonic crystal, but the

D. Felbacq, E. Rousseau
Laboratoire Charles Coulomb
Université de Montpellier and CNRS
Montpellier 34095, France
E-mail: didier.felbacq@umontpellier.fr

The ORCID identification number(s) for the author(s) of this article can be found under https://doi.org/10.1002/andp.202300321

DOI: 10.1002/andp.202300321

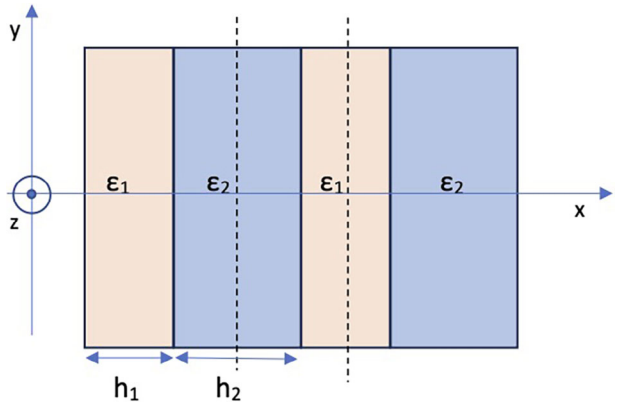

Figure 1. An example of 1D structure. It is a stratified photonic crystal with two homogeneous slabs in the basic cell. The vertical dashed lines correspond to the two origins for which the potential is symmetric.

results that we obtain apply to continuously varying structures, as well as to acoustic structures and to quantum waves in a 1D potential. For definiteness, we proceed by using the vocabulary of electromagnetism in the following: However, we will occasionally use the word "potential" generically to designate the permittivity (permeability) or the quantum confining potential. With an abuse of notation, we will talk of the "potential $V(x)$" to denote generically these quantities. We will further make the hypothesis that there is an inversion symmetry in the medium, that is, an origin can be chosen in such a way that $V(x) = V(-x)$.

Let us briefly recall the theory of 1D media.[18] We consider time-harmonic fields (time-dependence of $e^{-i\omega t}$) that are invariant along the axes y and z and depend only on the variable x (see Figure 1). Since the medium under consideration is invariant along two directions of space, the electromagnetic field can be decomposed as a sum of two linearly polarized fields. Either the electric field is linearly polarized along z ($E_{||}$ case) or the magnetic field is linearly polarized along z ($H_{||}$ case). In both cases, we denote by $u(x)$ the function representing the field, that is, $E_z(x) = u(x)e_z$ ($E_{||}$ case) or $H_z(x) = u(x)e_z$ ($H_{||}$ case). The medium is described by a periodic relative permittivity $\varepsilon(x)$ and a periodic relative permeability $\mu(x)$. The system of units is chosen in such a way that $\varepsilon(x+1) = \varepsilon(x)$, $\mu(x+1) = \mu(x)$. Let us consider the $E_{||}$ case, the $H_{||}$ case being obtained by switching ε and μ. The Maxwell–Faraday and Maxwell–Ampère equations provide the following relations

$$\nabla \times (ue_z) = i\omega\mu_0\mu H_z,\ \nabla \times H_z = -i\omega\varepsilon_0\varepsilon u e_z \tag{1}$$

which leads to

$$\nabla \times (\mu^{-1}\nabla u \times e_z) = k_0^2 \varepsilon u e_z \tag{2}$$

where $k_0^2 = (\omega/c)^2$. Projecting on e_z, we get

$$-\frac{d}{dx}\left(\mu^{-1}\frac{d}{dx}u\right) = k_0^2\varepsilon u \tag{3}$$

Finally, the following equation is obtained

$$Hu = k_0^2 u \tag{4}$$

where:

$$H = -p^{-1}(x)\frac{d}{dx}\left(q^{-1}(x)\frac{d}{dx}\right) \tag{5}$$

and, according to the polarization

$$E_{||}: q(x) = \mu(x),\ p(x) = \varepsilon(x),\ H_{||}: q(x) = \varepsilon(x),\ p(x) = \mu(x) \tag{6}$$

This equation is more conveniently rewritten as an order one differential system

$$\frac{d}{dx}U = \begin{pmatrix} 0 & 1 \\ -k_0^2 p(x) & 0 \end{pmatrix} U \tag{7}$$

where

$$U = \begin{pmatrix} u \\ \frac{1}{q(x)}\frac{du}{dx} \end{pmatrix} \tag{8}$$

In the following, we denote

$$u' = \frac{1}{q(x)}\frac{du}{dx} \tag{9}$$

From the general theory of ordinary differential equation,[19] there exists a so-called "resolvent matrix" $\mathcal{R}(x,y)$ such that $U(x) = \mathcal{R}(x,y)U(y)$.

Over one period, the values of $U(1)$ and $U(0)$ are related by the so-called "monodromy matrix"

$$\mathcal{M}(k_0) = \mathcal{R}(1,0) \tag{10}$$

This matrix is unimodular (i.e., $\det \mathcal{M} = 1$) and, as we will show, it characterizes the band structure in the Hermitian case. The monodromy matrix depends on the norm of the wavevector in vacuum (or on the energy of the system in the case of quantum physics). The characteristic polynomial of $\mathcal{M}$ reads as: $X^2 - tr(\mathcal{M})X + 1$, therefore three sets can be defined according to the nature of the eigenvalues of $\mathcal{M}$[20,21]

- $G = \{k_0 \in \mathbb{R},\ |\mathrm{Tr}(\mathcal{M}(k_0))| > 2\}$, for which the eigenvalues are real and inverse one of the other. This corresponds to non progagative modes, that is, band gaps.
- $B = \{k_0 \in \mathbb{R},\ |\mathrm{Tr}(\mathcal{M}(k_0))| < 2\}$, for which the eigenvalues are complex of modulus one and conjugated. This corresponds to progagative modes, that is conduction bands. The eigenvalues can be written $e^{\pm i\theta}$, with $\theta \in [-\pi, +\pi]$ the Bloch number and the interval $[-\pi, +\pi]$ is the so-called Brillouin zone.
- $\Delta = \{k_0 \in \mathbb{R},\ |\mathrm{Tr}(\mathcal{M}(k_0))| = 2\}$, for which the eigenvalues are ± 1. The eigenvalues are of multiplicity 2. We denote Δ_0 the subset of Δ for which $\mathcal{M}(k_0) = \pm I_d$.

Conventionaly, Bloch waves are associated to eigenvalues of modulus one and therefore, to propagative modes in the structure. This corresponds to the set B. Looking at the various sets, we see that the distinction between the various domains is purely qualitative: eigenmodes always exist in the system but they are unbounded for $k_0 \in G$. That is why we call "generalized Bloch modes" the modes corresponding to the sets G and Δ. In the

band gaps, the solutions to the wave equation are not bounded over the infinite structure, but they play a crucial role in the case of a finite or semi-infinite medium. We therefore take as a parameter the wavenumber k_0 that will vary in $\mathbb{R}^+$ and study the evolution of eigenvalues and eigenvectors with respect to k_0.

For $k_0 \in B$ and $\theta \in [-\pi, \pi]$, the fields that can exist in the structure are superposition of Bloch waves $\psi(x; \theta, k_0)$. The Bloch wave are quasi-periodic in the x variable, that is, there are of the form

$$\psi(x; \theta, k_0) = e^{i\theta x} u(x; \theta, k_0) \tag{11}$$

where $u(x; \theta, k_0)$ is 1-periodic in the x variable: $u(x+1; \theta, k_0) = u(x; \theta, k_0)$.

It is convenient to transform the Brillouin zone into the circle $S^1 = \{z \in \mathbb{C}, |z| = 1\}$, that is, we associate to $\theta \in [-\pi, \pi]$ the complex number $z = e^{i\theta} \in S^1$. Any function defined on the interval $[-\pi, \pi]$ can be considered a function on S^1. From now on, the Bloch modes are thus denoted $u(x; z, k_0)$. To each value of z, we can associate a set of wavenumbers

$$k_{0,j}(z), j = 1 \ldots \tag{12}$$

where $k_{0,j}^2$ are the eigenvalues of H and for each of these wavenumbers a complex vector space of dimension 1. The collection of these vector spaces constitutes the Bloch bundle associated with the branch $k_{0,j}(z)$. As a function of θ, it is not obvious that $u(x; \theta, k_0)$ satisfies the condition that $u(x; \pi, k_0) = u(x; -\pi, k_0)$. However, it is a general result that for any 1D complex bundle over S^1, there exists a *continuous* function $z \in S^1 \to u(x; z, k_0)$[10] (such a function is called a "section" of the bundle). This does not mean that no topological effect is to be expected, as we will see below, because we have the additional hypothesis that the potential is symmetric.

Due to the fact that the Bloch waves depend on both the direct and indirect variables x and θ this representation of the Bloch bundle is not easy to handle. We present another, simpler, representation of the bundle.

In order to make the discussion less arid, we shall now give a numerical illustration of the concept that we deal with (the code, written in Matlab, is available upon request). We consider the case of a binary medium, where the period is made of two homogeneous layers of relative permittivity ε_1 and ε_2 and width d_1 and d_2 (see Figure 1). Let us denote $\nu_j = \sqrt{\varepsilon_j}$, $j = 1, 2$.

For each layer, the monodromy matrix has the form

$$\mathcal{M}_j = \begin{pmatrix} \cos(k_0 \nu_j d_j) & \frac{1}{k_0 \nu_j} \sin(k_0 \nu_j d_j) \\ -k_0 \nu_j \sin(k_0 \nu_j d_j) & \cos(k_0 \nu_j d_j) \end{pmatrix} \tag{13}$$

and the complete monodromy matrix is simply $\mathcal{M} = \mathcal{M}_2 \mathcal{M}_1$. The dispersion relation is obtained by computing the trace of $\mathcal{M}$, which leads to the equation:

$$\cos(\theta) = \cos(k_0 \nu_1 d_1) \cos(k_0 \nu_2 d_2) - \frac{1}{2}\left(\frac{\nu_2}{\nu_1} + \frac{\nu_1}{\nu_2}\right) \sin(k_0 \nu_1 d_1) \sin(k_0 \nu_2 d_2) \tag{14}$$

and the eigenvectors $U^{\pm}$ are obtained by diagonalizing the monodromy matrix $\mathcal{M}$. An example of a band structure is given in Figure 2 where the conduction bands are labeled as in Equation (12).

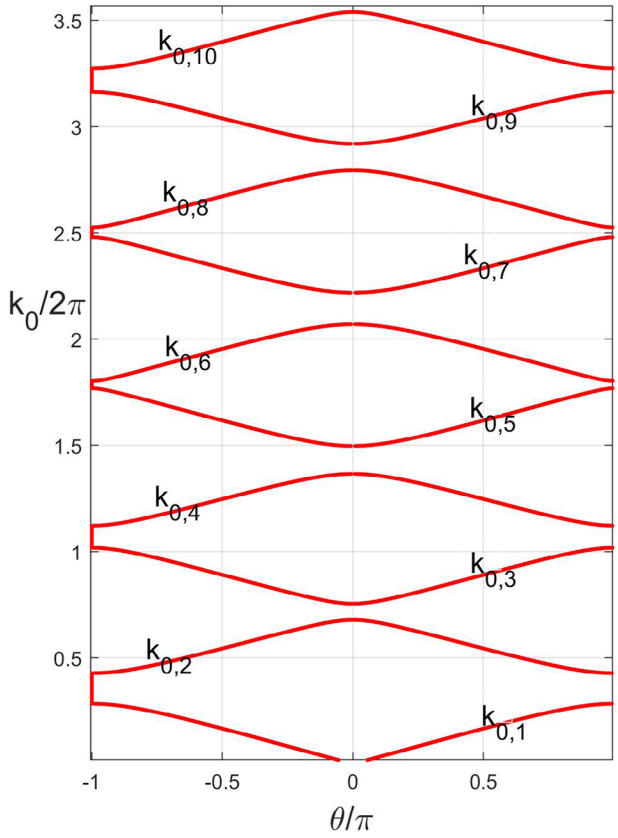

Figure 2. Band structure for a photonic crystal with parameters $\varepsilon_1 = 3.8$, $\varepsilon_2 = 1$, $h_1 = 0.42$, $h_2 = 0.58$ and the permeabilities are equal to 1. These are the values used in ref. [5]. The labeling of the branches is as in Equation (12).

Let us now extend this setting to complex values of the energies. Consider the Bloch variety

$$F = \left\{(z, k_0) \in \mathbb{C}^2, \exists\, U \neq 0 : \mathcal{M}(k_0) U = zU\right\} \tag{15}$$

The Bloch variety is obtained explicitly by computing the roots of the characteristic polynomial of $\mathcal{M}$

$$\det(\mathcal{M}(k_0) - zI_2) = 0 \tag{16}$$

This allows us to consider the situation when the potential is not necessarily real (i.e., the case of a non-Hermitian quantum system or of a media with losses). The Bloch variety defines the zeros set of an analytic function of the two variables (k_0, z). In the community of integrable systems, it is called the spectral curve of the system.[22] The vector bundle envisioned previously extends to a vector bundle over this curve. The situation of a real potential and real energies corresponds to the set $F_0 \subset F$ defined by

$$F_0 = \{(z, k_0) \in \mathbb{C} \times \mathbb{R}, \exists\, U \neq 0 : \mathcal{M}(k_0) U = zU\} \tag{17}$$

Generically, the monodromy matrix can be put in diagonal form. However, for $(k_0, z) \in \Delta \setminus \Delta_0$, a particular situation

happens: the eigenvalues ± 1 have a multiplicity of 2 but the eigenspace is of dimension 1. The points where this happens are called ramification points. The set Δ_0 where $\mathcal{M} = \pm I_2$ corresponds to a non-generic situation that is a topological phase transition, as will be shown in the following. Indeed, this corresponds to two bands touching at one point $z = \pm 1$. This singularity can be removed by an infinitesimal variation of the parameters. It separates two topological phases stable under small variations of the parameters far enough from this singularity.

3. Topological Characterization Using Poles and Zeros

Let us consider for now the usual case of a real potential, or lossless media. The eigenvectors $U^{\pm}(x_0)$ of $\mathcal{M}$ are the boundary values of the generalized Bloch waves at an origin x_0 that can be chosen at will. Changing the value of x_0 amounts to changing the basic cell to $[x_0, x_0 + 1]$. It is equivalent to a change of gauge in real space whenever an infinite medium is considered. When finite structures are considered, different choices of the origin will correspond to different physical properties, as shall be seen later on.

The eigenvectors $U^{\pm}$ are complex conjugated quantities, when the potential is real and for $k_0 \in B$. Using the resolvent matrix, the value of a Bloch mode at any point x in the period is obtained by using the relation: $U^{\pm}(x) = \mathcal{R}(x, x_0)\, U^{\pm}(x_0)$. From these considerations, we conclude that the Bloch eigenspace at a point (k_0, z) is entirely determined by the eigenvectors $U^{\pm}(x_0)$. Therefore, the Bloch bundle, that is, the collection of all the eigenspaces as z describes S^1, is isomorphic to the vector bundle of eigenvectors of the monodromy matrix $\mathcal{M}$. As we have already said, it is a complex vector bundle over S^1, and therefore it is trivial, which means that there exists a non-vanishing section, that is, a continuous parametrization of a Bloch mode all around the Brillouin zone. We recover here one of the conclusions of ref. [7]. Still, there can be topological properties provided that we take into account the hypothesis that the potential has an inversion symmetry σ: $V(x) = V(-x)$.

Two different origins, x_0 and x_1 can be chosen such that $V(x) = V(-x)$. These two points are such that $x_1 - x_0 = 1/2 \mod (1)$ (see Figure 1, where the two origins are indicated as dashed lines). Let us assume that the boundary values are chosen at one of the two points such that $V(x) = V(-x)$, that is, we fix the gauge in real space. This point is now the new origin, $x = 0$.

For the eigenvectors $U^{\pm}$ of the monodromy matrix $\mathcal{M}$, the inversion symmetry σ acts as $\sigma(U^{\pm}) = \sigma_z U^{\pm}$, where σ_z is the Pauli matrix $\begin{pmatrix} 1 & 0 \\ 0 & -1 \end{pmatrix}$. This is so because, under the change $x \to -x$, the derivative changes sign and the wave propagates backward; the corresponding monodromy matrix is $\mathcal{M}^{-1}$. The inversion symmetry implies that if U is an eigenvector of the monodromy matrix with the eigenvalue z then $\sigma_z U$ is an eigenvector of the monodromy matrix but with the eigenvalue $1/z$. As a consequence, we have the following result:

When $V(x) = V(-x)$, it holds:

$$\sigma_z \mathcal{M} \sigma_z = \mathcal{M}^{-1}, \text{ and the basis of eigenvectors is of the form } (U, \sigma_z U) \tag{18}$$

For $k_0 \in B$, it holds, projectively, $U^* = \sigma_z U$ ($*$ denotes complex conjugaison). When we say that two vectors are equal "projectively," we mean that they are collinear. Given a vector $U = (u(0; k_0, z), u'(0; k_0, z))^t$, the vector space generated by U is denoted $\tilde{\chi} = [u(0; k_0, z) : u'(0; k_0, z)]$. This is the standard notation for an element of the projective space $\mathbb{C}P_1$ which is the set of all complex lines going through the origin in the complex plane $\mathbb{C}^2$. This space is equivalent to the Riemann sphere, that is, the complex numbers $\mathbb{C}$ together with a point ∞ at infinity.

This suggests finding a function that characterizes an eigenspace. Given an eigenvector

$$U = (u(0; k_0, z), u'(0; k_0, z))^t \tag{19}$$

we define

$$\chi(k_0, z) = u(0; k_0, z)/u'(0; k_0, z) \tag{20}$$

This quantity does not depend upon the specific eigenvector that is chosen to represent the eigenspace, that is, for $\gamma \in \mathbb{C}$, the vectors U and γU define the same function χ.

For $k_0 \in B$, the ratio $\chi(k_0, z) = u(0; k_0, z)/u'(0; k_0, z)$ satisfies the relation $\chi^*(k_0, z) = -\chi(k_0, z)$ and therefore, thanks to Equation (18), it is purely imaginary in the conduction bands for a real potential.

For a given wavenumber k_0, there are two eigenvectors ($U^+ = U$, $U^- = \sigma_z U$) with eigenvalues z and $1/z$, respectively. Therefore two functions $\chi^{\pm}$ are obtained from the components of the eigenvector U^+ or U^-, respectively. These functions satisfy therefore the relation

$$\chi^+(k_0, z) = -\chi^-(k_0, 1/z) \tag{21}$$

Let us show that these can be combined to provide a single function.

For $k_0 \in G$, since one of the numbers $(|z|, 1/|z|)$ is lower than 1, we can define a single function χ such that

$$\chi(k_0) = \begin{cases} \chi^+(k_0, z), & |z| < 1 \\ -\chi^+(k_0, z), & |z| > 1 \end{cases} \tag{22}$$

In order to extend this definition to the conduction band, a criterium is needed to distinguish between z and $1/z$. Let us consider the functions: $k_0 \to z(k_0), k_0 \to 1/z(k_0)$, which represent the evolution of the eigenvalues as functions of k_0. The graphs of these functions are curves in the complex planes. This is represented in **Figures 3** and **4** when varying the wavenumber $k_0/2\pi$ between 0 and 4. These curves show all the possible eigenvalues for a given geometry. The parameters used for the calculations are indicated in the caption of Figure 2. The eigenvalues corresponding to propagating waves, that is, corresponding to the set B, lie on the unit circle. The eigenvalues corresponding to the band gap G have a null imaginary part. They give rise to the line segments around $z = \pm 1$. When the potential is real, the ramification points are 1 and -1. The curve in Figure 4 is the "blow-up" of the preceding curves by plotting directly the skew curve $k_0 \to (z(k_0), 1/z(k_0))$.

At the ramification point, the curves cross at a right angle, which makes it seemingly impossible to follow one eigenvalue

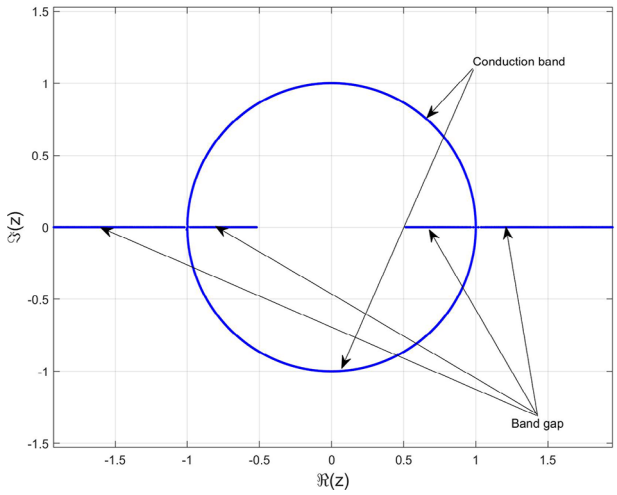

Figure 3. Eigenvalues of the monodromy matrix in the complex plane. The circle corresponds to B and the real intervals to G. The transitions between G and B, that is, the set Δ, correspond to $z = \pm 1$.

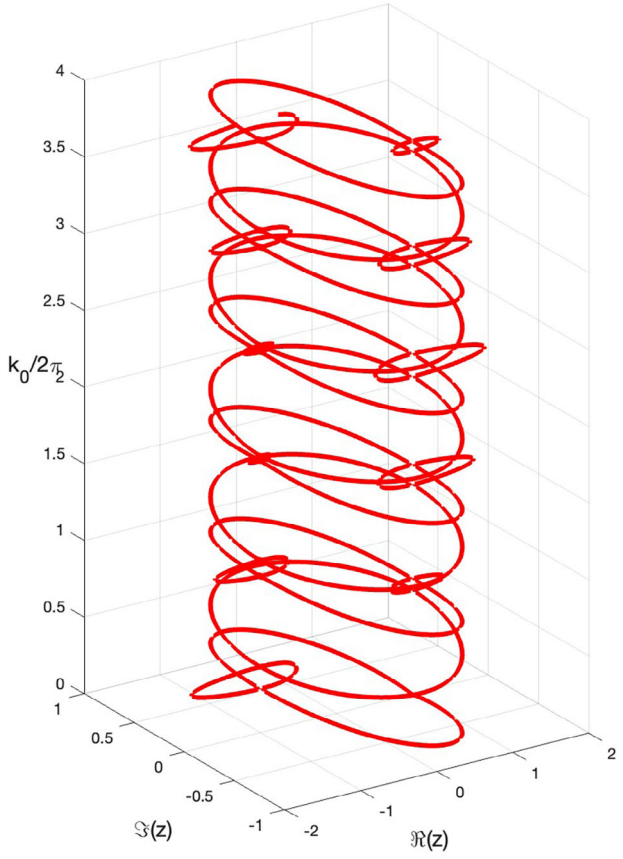

Figure 4. Evolution of the eigenvalues z as functions of k_0. The band gaps correspond to the (real) ovoid regions and the conduction bands to the helical parts of the curve.

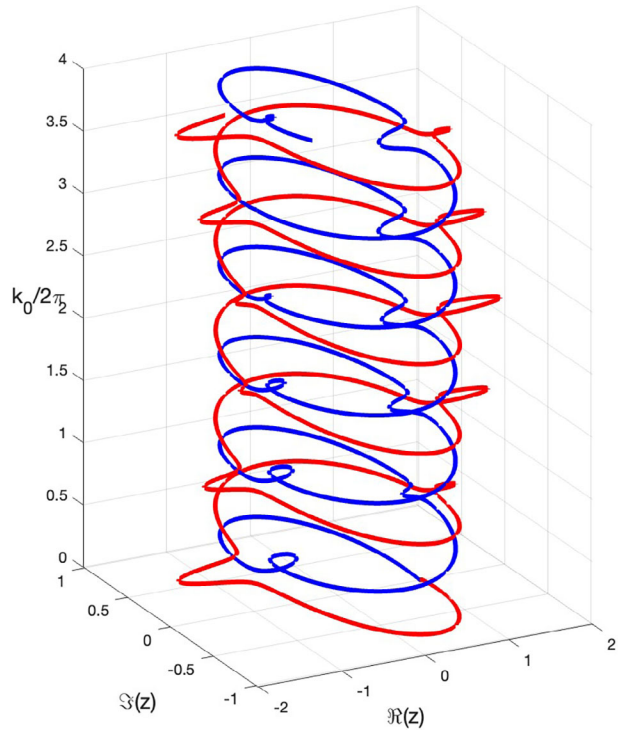

Figure 5. Evolution of the eigenvalues as functions of k_0 when at small imaginary part is added to k_0. The curves can now be distinguished (except at the bottom when $k_0 \to 0$): the blue curve corresponds to eigenvalues smaller than 1 in modulus within the band gaps and the red one to eigenvalues larger than 1 in modulus in the band gaps.

by continuity from B to G. However, this degeneracy is in fact directly linked to the stringent condition that the potential be real, since it is a consequence of the fact that the monodromy matrix has eigenvalues ± 1 at the boundaries of the conduction bands. This degeneracy can be lifted by using the limiting absorption principle, that is, by adding a small imaginary part δ either to the potential or to the frequency. Indeed, if we replace k_0 by $k_0 + i\delta$, the equation $tr(\mathcal{M}(k_0)) = \pm 2$ is replaced by the equation $tr(\mathcal{M}(k_0 + i\delta)) = \pm 2$. Therefore the crossing points are no longer real (generically). This is what is done in **Figure 5** where a small imaginary value of 10^{-2} was added to k_0. The real part of k_0 is used as a blow-up parameter to plot the eigenvalues as curves in $\mathbb{R}^3$. It is seen that the curves no longer cross and therefore the eigenvalues can be followed individually.

Since the eigenvalues can be distinguished, it is also possible to follow the eigenvectors by continuity, that is to resolve the ramification points. Therefore, the same holds for the functions $\chi^{\pm}$. For these functions, another extension problem appears when there is a pole. When a small imaginary part is added to k_0, the poles of $\chi^{\pm}$ gain a small imaginary part and the restrictions of these functions to the real axis of k_0 are now continuous. It is illustrated in **Figure 6** where the values of $\chi^{\pm}$ are plotted on the Riemann sphere by stereographic projection. We conclude the following:

There is a unique function $\chi(k_0, z)$ corresponding to eigenspaces associated with eigenvalues lower than 1 in modulus for $k_0 \in G$.

At the heart of the topological properties captured by the function χ are the poles and zeros that it possesses. A zero is

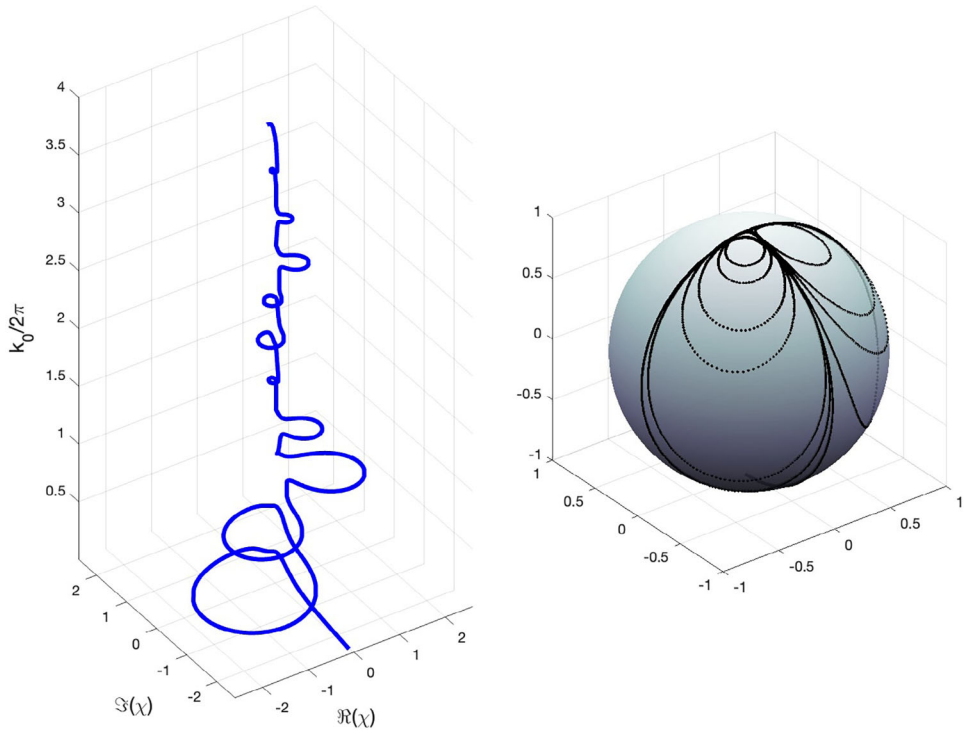

Figure 6. On the right, the graph of the function $\chi(k_0)$ on the Riemann sphere. The north pole corresponds to 0 and the south pole to infinity. On the left, the same but blowed up by using the parameter k_0.

associated with the eigenvector $(0,1)^t$ and a pole to the eigenvector $(1,0)^t$. We have the following result:

For $k_0 \in B$, since $U^*(k_0,z) = U(k_0,1/z)$, we have that either $\chi(k_0,z)$ is null at $z=\pm1$ or it has a pole.

The values of k_0 for which there can be a zero or a pole are characterized as follows. Assume that there is a zero k_Z in the interior of a band. Then $\chi^{\pm}$ are both null and therefore the eigenvectors of $\mathcal{M}(k_Z)$ are linearly dependent and the eigenvalues z and $1/z$ are equal. Consequently, $tr(\mathcal{M}) = \pm 2$. If $tr(\mathcal{M})$ is not transversal there, that is, if the derivative of $tr(\mathcal{M})$ is null, then it is a non-generic point that can be removed by an infinitesimal variation of the parameters. Similarly, if there is a pole of χ then $U = (1,0)^t$ with eigenvalue z. The other eigenvector is $\sigma_z U = (1,0)^t$. Therefore there is a degeneracy and $z^2 = 1$ and therefore $tr(\mathcal{M}) = \pm 2$. We can then conclude the following:

The only poles and zeros of the function χ are generically situated at band edges only, that is, at points where $tr(\mathcal{M}) = \pm 2$ and $\mathcal{M} \neq \pm I_2$. They are real when the potential is real.

The position of poles and zeros is the clue to understanding the topological properties of the structures. Indeed, a topological transition is characterized by the closing and re-opening of a gap through a continuous variation of the parameters defining the structure. The value of k_0 for which the lower and upper bands touch is a critical point of $f(k_0) = \mathrm{Tr}(\mathcal{M}(k_0))^2 - 4$, indeed, there it holds $f(z) = 0$ and $f'(z) = 0$. Therefore: $\mathcal{M} = \pm I_2$. Since at this point the eigenvectors are $(1,0)^t$ and $(0,1)^t$, this means that a pole and a zero of χ merge. As a consequence, there is always a pole and a zero at the boundaries of a band gap. In other words, when the topological transition takes place, a pole and a zero change places and therefore they have to merge. We conclude that:

When the potential is real, the topological transitions take place at $\mathcal{M} = \pm I_2$.

Furthermore, the poles and zeros are continuous functions of the parameters and disappear only when they merge. As a consequence:

The ordered sequence of poles and zeros is a topological invariant. It determines the positions of the forbidden and conduction bands

This sequence is called the poles and zeros pattern. For a given band gap, the various possibilities are zero–zero, zero–pole, pole–zero, pole–pole.

When losses are added, the situation is more complicated, because in that case the poles and zeros pattern is contained in the lower part of the complex plane. When the potential is complex, the function χ is no longer purely imaginary in the conduction bands nor real in the band gaps. It turns out that the function χ is defined over F and takes values in the projective space, assimilated to the Riemann sphere. This result is immediate whenever the eigenspaces are not degenerated, since the entries of the monodromy matrix are holomorphic.

4. The Berry–Zak Phase and the Triviality of the Bundle

Let us relate these results to the Berry–Zak phase. This phase is the one that is acquired by a Bloch wave as the Bloch number evolves around the Brillouin zone. It is defined explicitly as follows: Consider the periodic part of a Bloch mode $\psi(k;x)$. The Bloch mode infinitely close to $\psi(k;x)$ is obtained by making a small variation dk and by imposing that ψ is transported without variation at order 1. To do so, we write that $\psi(k+dk;x) =$

$\psi(k;x) + \partial_k\psi(x;k)dk + O(dk^2)$, and we impose that the variation $\delta\psi$ of ψ belongs to the eigenspace of ψ:

$$\delta\psi = \Pi_\psi\big(\psi(k+dk;x) - \psi(k;x)\big) \tag{23}$$

where $\Pi_\psi = |\psi\rangle\langle\psi|$. This gives: $\delta\psi = \langle\psi, \partial_k\psi\rangle\psi$. This defines the so-called "connection form:" $A(k) = \langle\psi, \partial_k\psi\rangle dk$. From this definition, it is seen that $A(k)$ is purely imaginary for a normalized Bloch mode. Indeed, if $\langle\psi,\psi\rangle = 1$, then $\langle\partial_k\psi,\psi\rangle + \langle\psi,\partial_k\psi\rangle = 0$.

For a generic Bloch mode $\phi(k;x) = w(k)\psi(k;x)$, the parallel transport of ϕ around the Brillouin zone amounts to let ϕ evolve in such a way that its variation is orthogonal to the the eigenspace generated by ψ (this is what is done in first order time-independent perturbation theory): $\langle\delta\phi,\psi\rangle = \partial_k w + A(k)w = 0$.[12] This gives the differential equation: $\partial_k w = -A(k)w$ and therefore: $w(k) = e^{-\int_{-\pi}^{k} A(k')}w(-\pi)$. Going around the Brillouin zone defines the so-called Berry–Zak phase $\int_{-\pi}^{\pi} A(k')$ through the integration of the differential equation: $w(\pi) = e^{-\int_{-\pi}^{\pi} A(k')}w(-\pi)$. A major result obtained in ref. [6] and re-expressed in terms of geometrical phases in ref. [7] is that, provided the potential as the invertion symmetry, it holds:

$$e^{-\int_{-\pi}^{\pi} A(k')} = \pm 1. \tag{24}$$

The Bloch bundle is trivial when the value is 1 and non-trivial when it is -1. This is equivalent to the existence of an *equivariant section*. Here, equivariant means that a section, that is, a continuous parametrization of a Bloch mode over the Brillouin zone, satisfies a compatibility condition with the inversion symmetry.

This concept translates easily in our formulation. Indeed, the Bloch modes are represented by the eigenvectors of $\mathcal{M}(k_0)$ and a conduction band corresponds to an interval of wavenumbers $[k_1, k_2]$. At the boundaries k_1, k_2 the monodromy matrix is of one of the following form

$$\begin{pmatrix} \pm 1 & * \\ 0 & \pm 1 \end{pmatrix} \text{ or } \begin{pmatrix} \pm 1 & 0 \\ & \pm 1 \end{pmatrix} \tag{25}$$

where $*$ is a non-zero element. The corresponding eigenvectors are

$$\begin{pmatrix} 1 \\ 0 \end{pmatrix}, \begin{pmatrix} 0 \\ 1 \end{pmatrix} \tag{26}$$

The point, however, is the possibility to follow by continuity an eigenvector around the Brillouin zone. As already said, since the bundle is complex and over S^1, such a section necessarily exists.[10] Here, we request further that it be equivariant, that is, that it be compatible with the group action induced by the inversion symmetry. Specifically, an equivariant section $V(k_0, z)$ should satisfy

$$U(k_0, 1/z) = \tilde{\sigma}\, U(k_0, z) \tag{27}$$

where

$$\tilde{\sigma} = \sigma_z \text{ or } \tilde{\sigma} = -\sigma_z \tag{28}$$

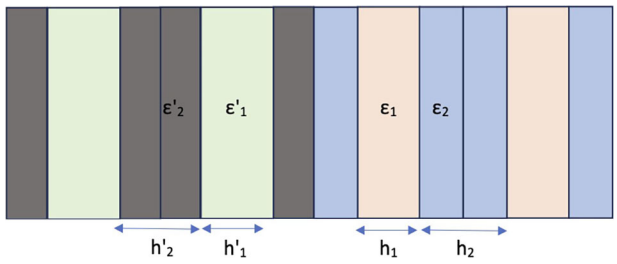

Figure 7. The structure is made with two 1D photonic crystals with different topological properties.

- Assume that we start with the eigenvector $(1,0)^t$ (that is, a pole of χ) for $z = 1$. It satisfies the relation: $(1,0)^t = \sigma_z(1,0)^t$. Let us say that we follow the upper part of S^1, then we arrive at an eigenvector $(a,b)^t$ for $z = -1$ that corresponds either to a zero or to a pole. Going around the lower part, we arrive at the eigenvector $(a',b')^t$ for $z = -1$. Keeping into account the equivariance of the section, we impose that $(a',b')^t = \sigma_z(a,b)^t$, that is: $a = a'$, $b = -b'$. For the section to be continuous, we have, of course to impose: $a = a'$, $b = b'$, but then, of course, $b = 0$. Therefore we end up with the eigenvector $(1,0)^t$. We have therefore fulfilled the conditions for the existence of a section.
- Let us start now with a zero $(0,1)^t$. This does fulfill the requirement of equivariance provided that we write $(0,1)^t = -\sigma_z(0,1)^t$. If there is also a zero at $z = -1$, the same gluing works to provide a global section.
- The situation is different if we start with a zero $(0,1)^t$ and end with a pole $(1,0)^t$. This time we start with the condition $(0,1)^t = -\sigma_z(0,1)$ and end with the condition $(1,0)^t = \sigma_z(1,0)^t$. Therefore, the section is not globally equivariant and it has to be twisted.

We end up with the following conclusions:

1) *The pole–pole or zero–zero cases correspond to a Berry phase equals to 0,*
2) *The pole–zero or zero–pole cases correspond to a Berry phase equals to π.*

We note that following our approach, the Berry–Zak phase is very easy to compute, as it suffices to consider the form of the monodromy matrix at the boundaries of the conduction bands.

5. The Bulk-Boundary Correspondence

Let us consider a structure made of two semi-infinite photonic crystals, Phc1 and Phc2, put side by side, such as depicted in **Figure 7**, and characterized by the monodromy matrices $\mathcal{M}_1$ and $\mathcal{M}_2$. Our point is to investigate under what conditions a boundary mode can exist and how it can be characterized topologically by means of the properties of the χ function.

The edge states are ruled by the following result. Assume the photonic crystal Phc1, defined by $\mathcal{M}_1$, extends over $x < 0$ and that Phc2, defined by $\mathcal{M}_2$, extends over $x > 0$. At k_0 the eigenvalues of $\mathcal{M}_1$ and $\mathcal{M}_2$ are real and of the form $(z_1, 1/z_1)$ and $(z_2, 1/z_2)$. Let us assume that $|z_{1,2}| < 1$. A boundary mode is characterized

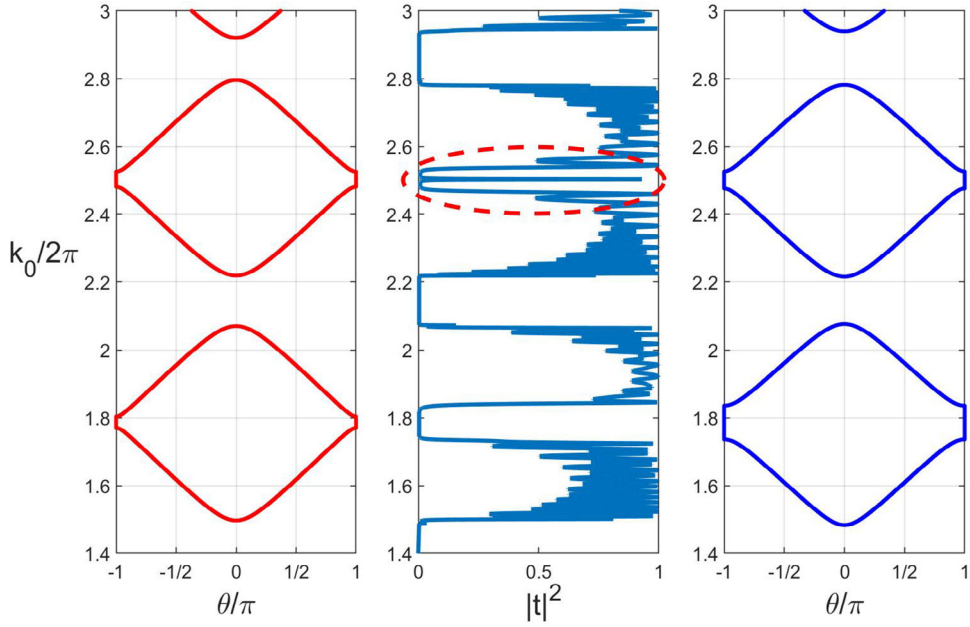

Figure 8. Band structures for two photonic crystals with parameters $\varepsilon_1 = 3.8$, $\varepsilon_2 = 1$, $h_1 = 0.42$, $h_2 = 0.58$ (Phc1), on the left, and $\varepsilon_1 = 4.2$, $\varepsilon_2 = 1$, $h_1 = 0.38$, $h_2 = 0.62$ (Phc2), on the right. The origin is chosen in such a way that the basic cell contains three layers of width $h_1/2$, h_2, $h_1/2$, and permittivities ε_1, ε_2, and ε_1. In both cases the permeabilities are equal to 1. In the middle the transmission spectrum is given. It is obtained with a finite structure comprising ten periods of each photonic crystal. The peak inside the band gap (highlighted by a red dashed ellipsis) corresponds to an edge mode.

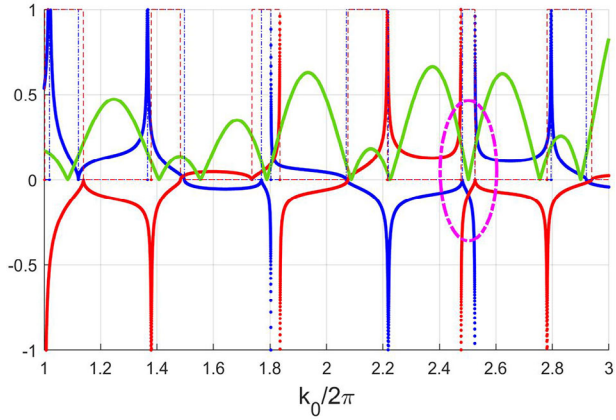

Figure 9. In red the function χ_1, in blue the function $-\chi_2$. The commutator of $\mathcal{M}_1$ and $\mathcal{M}_2$ is plotted in green. The positions of the band gaps are indicated by the red dashed curve for Phc1 and the blue dot-dashed curve for Phc2 (the value of 1 corresponds to the band gaps and 0 to the conduction bands). The edge mode appears when χ_1 and $-\chi_2$ cross. As explained in the text, the commutator is null when χ_1 and $-\chi_2$ cross (indicated by the dashed ellipsis).

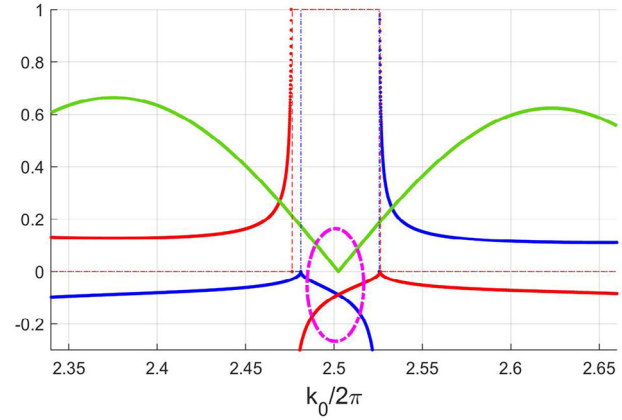

Figure 10. Same as Figure 9 but zoomed in.

by its initial value U at the junction between the media. For the mode to be bounded, the vector U should be damped along $x > 0$ and $x < 0$, therefore it should hold

$$\mathcal{M}_1 U = 1/z_1 U \text{ and } \mathcal{M}_2 U = z_1 U \tag{29}$$

This means first that, generically, $\mathcal{M}_1$ and $\mathcal{M}_2$ have a common set of eigenvectors, hence these matrices commute. Second, because of the symmetry of the potential, the second eigenvector is $V = \sigma_z U$.

We can thus conclude the following:

Let $\mathcal{M}_1$ and $\mathcal{M}_2$ be the respective monodromy matrices of each photonic crystal Phc1 and Phc2. For a Bloch wavevector k_0, there exists an eigenvector vector $U(k_0)$ defining an edge state provided the following conditions are fulfilled:

- *The matrices $\mathcal{M}_1(k_0)$ and $\mathcal{M}_2(k_0)$ have a common gap at the Bloch wavevector k_0, that is, $|\mathrm{tr}(\mathcal{M}_1)| > 2$ and $|\mathrm{tr}(\mathcal{M}_1)| > 2$.*
- *The matrices $\mathcal{M}_1(k_0)$ and $\mathcal{M}_2(k_0)$ commute:$[\mathcal{M}_1(k_0), \mathcal{M}_2(k_0)] = 0$.*

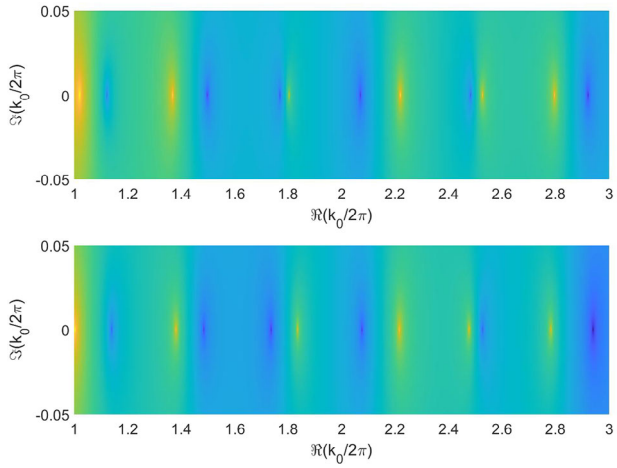

Figure 11. Poles and zeros patterns for the two photonic crystals described in Figure 8. The bright spots are the poles and the blue ones the zeros. Around the value $k_0/2\pi = 2.5$ one of the photonic crystal (top figure, corresponding to Phc1) has a zero–pole pattern while the other one (bottom figure, corresponding to Phc2) has a pole–zero pattern.

- *The associated Bloch functions* $\chi_1(k_0)$ *and* $\chi_2(k_0)$ *have opposite signs.*

The last two conditions are equivalent to the single following one:

- *The values of the Bloch functions* $\chi_1(k_0)$ *and* $\chi_2(k_0)$ *are opposite*: $\chi_1(k_0) = -\chi_2(k_0)$.

The link with the poles and zeros pattern can now be deduced. Recall that at the boundaries of the gaps the functions χ necessarily have a zero or a pole and that they have a constant sign within a band gap. This means that, provided χ_1 and χ_2 have opposite signs in a band gap, when the pattern inside a gap is pole–zero for one structure and zero–pole for the other, the functions χ_1 and $-\chi_2$ necessarily cross and there is necessarily an edge mode.

A few words are in order as to the fact that the existence of a mode is linked in a very strict way to the symmetry property of the potential, as far as the theoretical analysis is concerned. An edge mode inside a gap corresponds to a pole of the scattering matrix (i.e., of the reflection and the transmission coefficients). Since we expect the pole to be a continuous function of the parameters it seems paradoxical that it could disappear suddenly when the symmetry is broken since it can be broken in a continuous fashion by moving continuously the origin of the basic cell. To resolve this apparent paradox, one should recall that the reflection and transmission coefficients are defined for two finite structures put side by side (see ref. [21] for the definition of the reflection coefficient for a semi-infinite photonic crystal). When two semi-infinite photonic crystals are considered, the mode should be evanescent in both photonic crystals away from the edge and this is a strict condition. When finite photonic crystals are considered (containing each N periods), and with an plane wave incident field, there necessarily are anti-evanescent waves in addition to evanescent waves in order to fulfill the boundary conditions. Therefore, breaking the symmetry condition does not kill suddenly the edge mode, rather its wavenumber is shifted toward the edges of the band gap and, as the number of periods N tends to infinity, the edge mode disappears continuously by being absorbed at the edges of the band gap.

Let us illustrate these results numerically. The two band structures corresponding to each photonic crystal are given in **Figure 8**. A finite structure made of 10 periods of each photonic crystal is considered. The transmission spectrum for an incident plane wave is plotted in Figure 8. The existence of an edge state

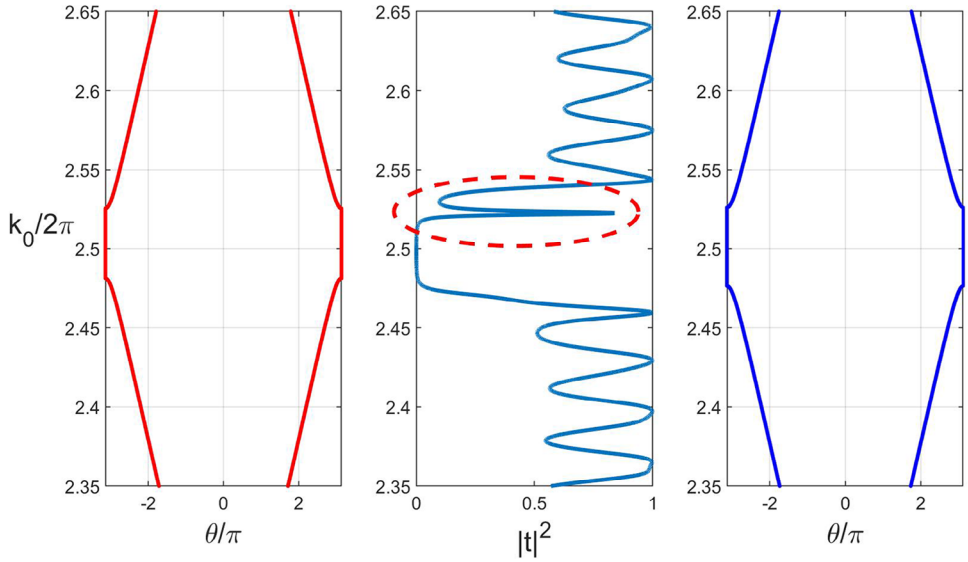

Figure 12. Band structures for the same photonic crystals as in Figure 8 but the photonic crystal on the left (Phc2) no longer satisfies the symmetry condition. The formula for the widths of the layers of the basic cell is now $3/5h_1, h_2, 2/5h_1$ and the permittivities are $\varepsilon_1, \varepsilon_2, \varepsilon_1$. In the middle, the transmission spectrum is given. An edge mode is still present (corresponding to the peak enclosed by the dashed red ellipsis) but it has moved toward the upper edge of the bandgap.

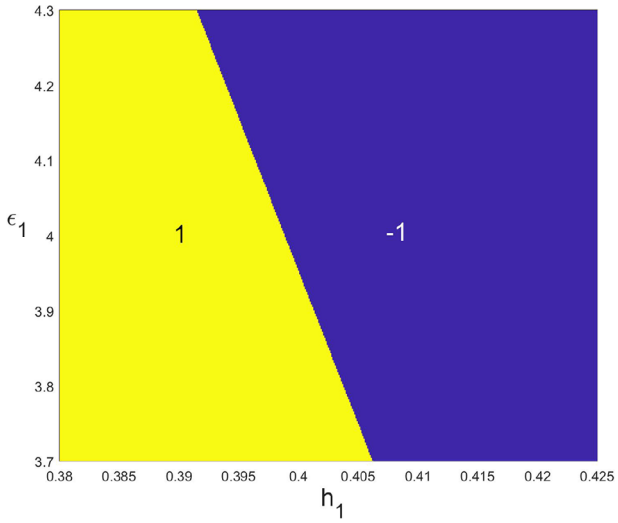

Figure 13. Phase diagram for a stratified medium with two slabs. The parameters are the permittivities $\varepsilon_{1,2}$ and the widths $h_{1,2}$ of the slabs. Since the period is 1, there is only one width parameter since $h_1 + h_2 = 1$. We fix $\varepsilon_2 = 1$ and the only permittivity parameter is ε_1. The diagram corresponds to the existence of a band gap in the interval [2.4; 2.6]. The index 1 is attributed to the pattern pole–zero and the index −1 to the pattern zero–pole.

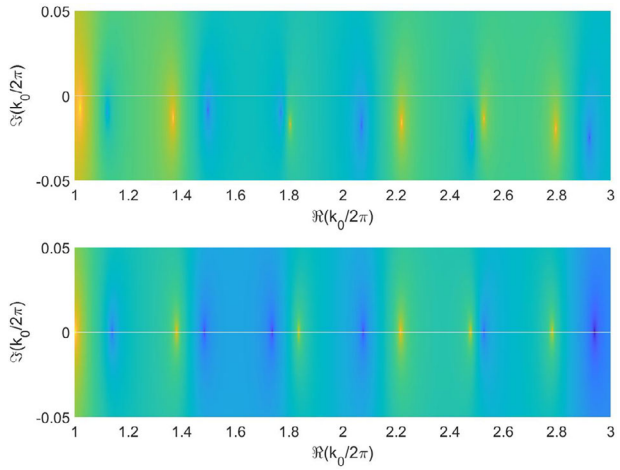

Figure 14. Same as Figure 11, but losses have been added to the photonic crystal Phc1, corresponding to the figure at the top. The other photonic crystal Phc2 remains lossless. For Phc1, the poles and zeros pattern is still there, except that, due to the presence of losses, the poles and zeros have moved toward the lower part of the complex plane of wavevectors. It can still be seen that the band gap around $k_0/2\pi = 2.5$ corresponds to a pole–zero/zero–pole pattern.

is detected as a peak inside the band gap for the forbidden band situated inside the interval of $k_0/2\pi \in [2.4, 2.6]$.

In **Figures 9** and **10**, we have plotted χ_1 (in red) and $-\chi_2$ (in blue), as well as the commutator of $\mathcal{M}_1$ and $\mathcal{M}_2$ in green. The positions of the band gaps are indicated by the dashed blue and dot-dashed red curves (with a value of 1 in the band gaps and 0 in the conduction bands). As can be seen in Figures 9 and 10, the edge state (appearing as a peak inside the band gap in the transmission spectrum, cf. Figure 8) corresponds to a value of k_0 for which the functions χ_1 and $-\chi_2$ cross and the commutator of the monodromy matrices is null. All the other zeros of the commutator do not correspond to a crossing of χ_1 and $-\chi_2$.

Let us now see what happens when complex values of k_0 are used. In **Figure 11**, we plot the absolute value of χ in the complex strip around the real axis. The poles are indicated by bright spots and the zeros by blue spots. We see clearly that both photonic crystals have the same poles and zeros pattern, except for the gap around $k_0/2\pi = 2.5$ where one of the structure has the pattern zero–pole and the other one the pattern pole-zero. In this band gap, there is a boundary mode. In **Figure 12**, we have plotted the band structure and transmission spectrum when the right-hand side photonic crystal does not fulfill the symmetry condition that $V(-x) = V(x)$. As explained in the discussion above, the edge mode is still present but is shifted toward the boundary of the band gap. By varying the values of the permittivities and the width of the layers, it is possible to obtain a phase diagram for the topological properties, that is, the poles and zeros pattern (cf. **Figure 13**). It can be seen that the regions of interest are separated by a line corresponding to the closing of the band gap.

Our point is now to study the situation where the potential is complex, that is, an imaginary part is added to the permittivities.

The new poles and zeros pattern is given in **Figure 14** for both the photonic crystals Phc1 and Phc2, as defined in Figure 8 but

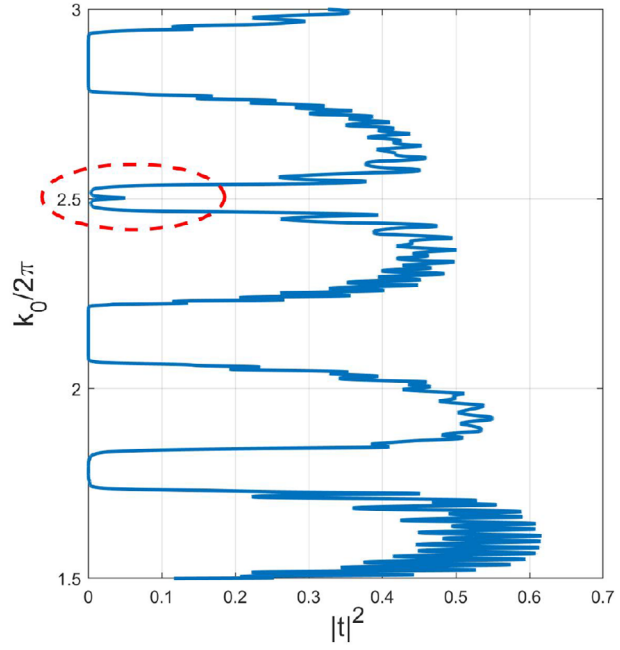

Figure 15. Transmission spectrum for the finite structure made of two finite photonic crystals containing ten periods and put side by side as defined in Figure 14. Losses are present in the finite Phc1, but there is still an edge mode. It appears as a peak inside a band gap. Due to the losses, the peak is larger and the maximum value is smaller than in Figure 8.

with a small imaginary part of 0.01 added to the permittivities of the layers of Phc1 (Phc2 remains lossless). There, it can be seen that the poles and zeros have moved toward the lower part of the complex plane of wavevectors. Still, the poles and zeros pattern is preserved. There is a continuous transformation, mathematically speaking, a homotopy, between the poles and zeros

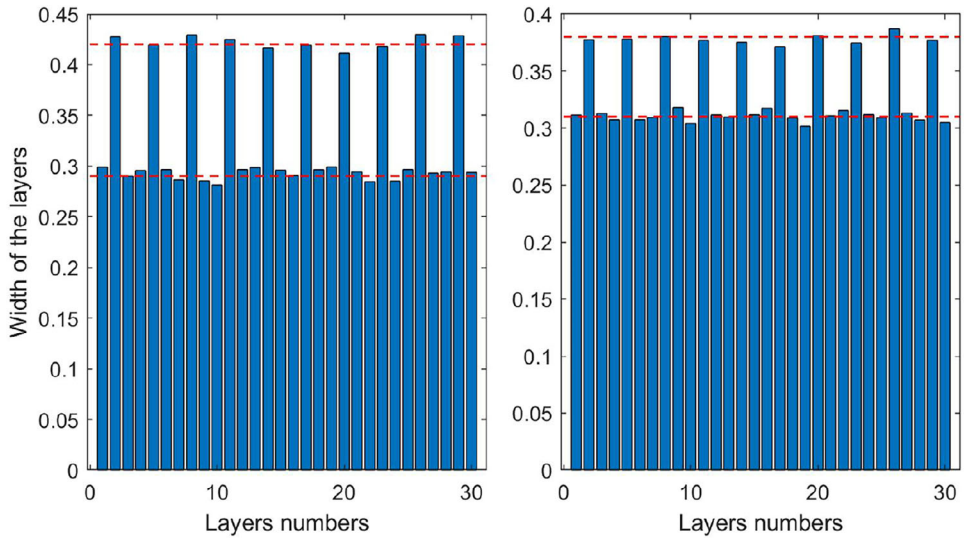

Figure 16. The figure represents the widths of the layers for one realization of the structure with some disorder. We have represented the widths of each of the 30 layers of each of the two photonic crystals put side by side. The figure on the left corresponds to Phc1 and the figure on the right corresponds to Phc2. The dashed red lines indicate the widths of the layers when there is no disorder, that is, the values given in Figure 8.

structures of both photonic crystals. When a pole and zero exchange places by continuously varying a parameter, there is a configuration for which the pole and the zero have the same real part. This amounts to saying that the gap closes there. Consequently, as far as the poles and zeros pattern remains close to the real axis, these patterns continue to characterize topologically the structures. Indeed, when plotting the transmission spectrum for the finite structure with losses (cf. **Figure 15**), a mode can be seen to remain (as an enlarged peak) in the same band gap. Of course, the life-time of the mode is now much shorter due to material losses added to radiative losses.

6. Conclusion and Possible Extensions

It is customary to analyze the topological properties of one dimensional structures by using the familiar concept of the Zak phase, directly linked to Berry's connection. We have shown here that another approach can be put forward, by using the poles and zeros of a function defined for all energies and not only for that corresponding to propagating modes. By using this tool, the extension of the topological classification of Bloch waves to lossy or non-Hermitian situations is straightforward and avoids the difficulties encountered when trying to extend the Berry connection

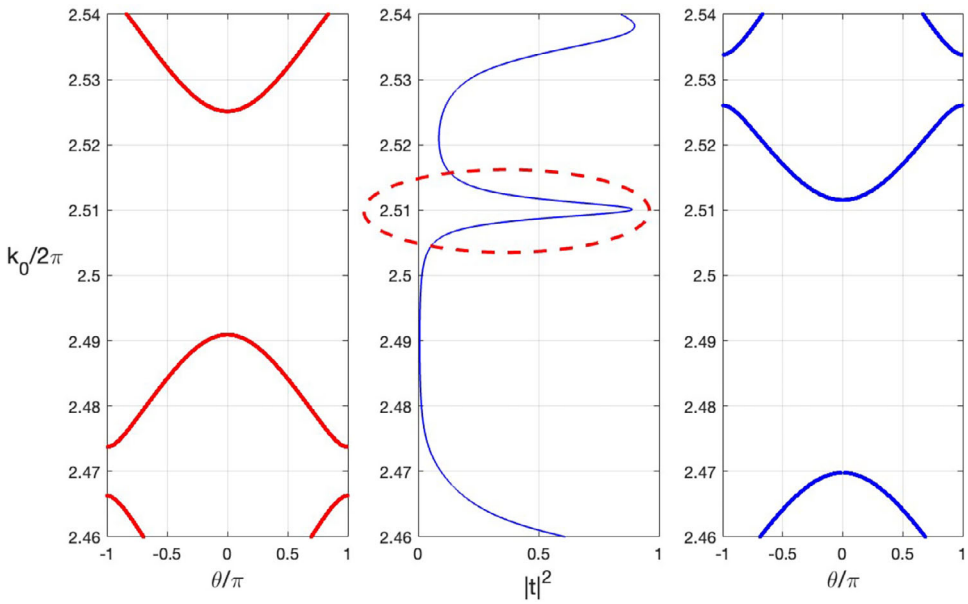

Figure 17. The left most and right most figures represent the Bloch diagram for the disordered photonic crystals. The middle figure represents the transmission spectrum for the complete structure. A peak corresponding to an edge mode can be seen (dashed red ellipsis). The onset of this mode is analyzed in Figure 18.

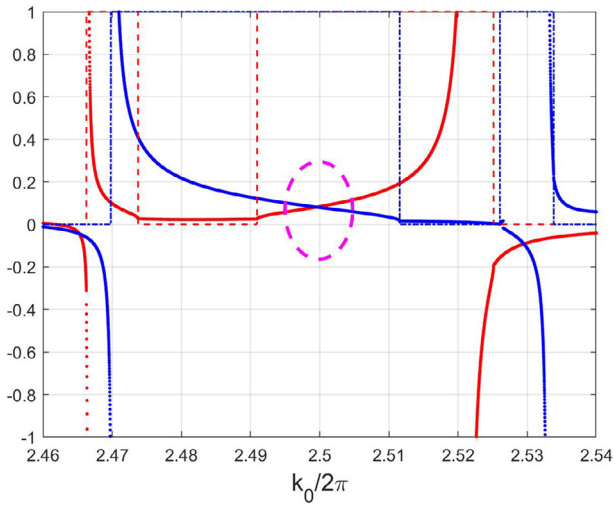

Figure 18. The figure represents the functions χ_1 (in red) and $-\chi_2$ (in blue). It is seen that the peak in the transmission curve of Figure 17 corresponds to different patterns of poles and zeros of the functions χ_1 and χ_2: it is a zero–pole pattern for χ_1 and a pole–zero pattern for χ_2.

approach to non-Hermitian systems. Moreover, our approach can be applied to structures in which a small amount of disorder is introduced. While a complete exposition goes beyond the scope of this work, let us give one numerical example. The structure is the same as that used in the previous simulations and defined in Figure 8, but a small amount of disorder is now added to the widths of all the layers. More precisely, we start with ten periods of the three-layers structure and then we add some disorder to the width of the layers. The disorder is obtained by modifying the width of the layers by an amount of ± 0.01 at most with a uniform law. We thus deal with 30 layers for each structure. The entire structure contains 60 layers. A typical realization of the media is given in **Figure 16**.

The monodromy matrix is now computed by taking into account the entire structure since the periodicity is lost. The Bloch diagrams and the transmission spectrum are given in **Figure 17**.

The functions χ_1 and χ_2 are given in **Figure 18**.

A mode is obtained as can be seen in Figure 17: A peak is seen inside the transmission spectrum around $k_0/2\pi = 2.5$ inside a common band gap of both photonic crystals. In this bang gap, the curves χ_1 and $-\chi_2$ cross with inverted pole and zero patterns (see Figure 18). This shows that the method also works in that situation.

A natural question is to investigate whether it is possible to extend this approach to higher dimensional structures. It is a general rule that the methods employed in dimension 1 are difficult to extend to dimensions 2 or 3. While the extension of our approach seems difficult to extend to higher dimensions for continuous models, the situation seems more accessible when considering tight-binding models, where the proposed approach could give possible theoretical insights for handling the case of complex energies and for analyzing the Bloch variety.[23] By tight-binding model, we have in mind a structure such as an inverted contrast 2D photonic crystal where holes are filled in such a way as to design a periodic superstructure made of weakly coupled cavities. We are currently investigating the properties of such a structure which is amenable to a discrete description.

Conflict of Interest

The authors declare no conflict of interest.

Data Availability Statement

The data that support the findings of this study are available from the corresponding author upon reasonable request.

Keywords

photonic crystals, topological properties, wave physics

Received: July 7, 2023
Revised: October 20, 2023
Published online:

[1] T. Ozawa, H. M. Price, A. Amo, N. Goldman, M. Hafezi, L. Lu, M. C. Rechtsman, D. Schuster, J. Simon, O. Zilberberg, I. Carusotto, *Rev. Mod. Phys.* **2019**, *91*, 015006.
[2] M. Z. Hasan, C. L. Kane, *Rev. Mod. Phys.* **2010**, *82*, 3045.
[3] Z. Wang, Y. Chong, J. D. Joannopoulos, M. Soljacic, *Nature* **2009**, *461*, 772.
[4] L.-H. Wu, *Phys. Rev. Lett.* **2015**, *114*, 223901.
[5] M. Xiao, Z. Q. Zhang, C. T. Chan, *Phys. Rev. X* **2014**, *4*, 021017.
[6] W. Kohn, *Phys. Rev.* **1959**, *115*, 809.
[7] J. Zak, *Phys. Rev. Lett.* **1989**, *62*, 2747.
[8] B. Simon, *Phys. Rev. Lett.* **1983**, *51*, 2167.
[9] M. V. Berry, *Proc. R. Soc. Lond. A* **1984**, *392*, 45.
[10] C. Nash, Charles, S. Sen, *Topology and Geometry for Physicists*, Academic Press Inc., San Diego **1987**.
[11] M. Nakahara, *Geometry, Topology and Physics*, IOP, Bristol **1990**.
[12] X.-R. Wu-Morrow, C. Dewitt-Morette, L. Rozansky, *Int. J. Mod. Phys. B* **1997**, *11*, 1389.
[13] N. Okuma, M. Sato, *Annu. Rev. Condens. Matter Phys.* **2023**, *14*, 83.
[14] S. Lieu, *Phys. Rev. B* **2018**, *97*, 045106.
[15] H. Shen, B. Zhen, F. Liang, *Phys. Rev. Lett.* **2018**, *120*, 146402.
[16] K. Kawabata, K. Shiozaki, K. Ueda, M. Sato, *Phys. Rev. X* **2019**, *9*, 041015.
[17] M. G. Silveirinha, *Phys. Rev. B* **2019**, *99*, 125155.
[18] D. Felbacq, B. Guizal, F. Zolla, *Opt. Commun.* **1998**, *152*, 119.
[19] V. I. Arnold, *Ordinary Differential Equations*, Springer, Berlin **2006**.
[20] R. Smaali, D. Felbacq, G. Granet, *Phys. E* **2003**, *18*, 443.
[21] G. Bouchitté, D. Felbacq, Didier, F. Zolla, *Wave Motion* **2005**, *42*, 75.
[22] O. Babelon, D. Bernard, M. Talon, *Introduction to Classical Integrable Systems*, Cambridge University Press, Cambridge **2003**.
[23] D. Gieseker, H. Knoerrer, E. Trubowitz, *The Geometry of Algebraic Fermi Curves*, Academic Press, San Diego, CA **1993**.